Proceedings of the 3rd International Congress APMAS2013, April 24–28, 2013, Antalya, Turkey

Structural Characterization of Al_2O_3 and CeO_2 Supported Ni, Co Loaded Ceramic Monolithic Catalysts

N.Ö. Guldal* and S.Z. Baykara

Chemical Engineering Dept., Yildiz Technical University, Topkapi, Istanbul 34210, Turkey

This paper discusses structural characterizations of monolithic catalysts prepared by incorporating Ni and Co supported over a porous alumina and ceria layer by using respective nitrates and H_2PtCl_6 as precursors. Monolithic catalysts were synthesized by dip-coating of 400 cpsi cordierite ceramic monolithic pieces cut in 20×13 mm^2 ($L \times D$) into appropriate solutions of metals, followed by calcination in air at 800 °C for 4 h. Phases of catalysts were characterized with X-ray diffraction. Morphological analysis and elemental composition were determined by scanning electron microscope and energy dispersive spectroscopy. The specific surface area analysis have been studied using the Brunauer–Emmett–Teller method. Metal contents were determined by inductively coupled plasma optical emission spectrometry.

DOI: 10.12693/APhysPolA.125.281

PACS: 81.15.−z, 81.70.−q, 82.65.+r

1. Introduction

Hydrogen is a nonpolluting and renewable fuel especially when it is used in fuel cells and it does not occur substantially in elemental form in nature, hence it has to be produced from various sources like water, fossil fuels, biomass and hydrogen sulfide (H_2S); a waste gas is another potential source. There are diverse technologies upon hydrogen production. One of those is based on hydrocarbon reforming which includes natural gas, gasoline, diesel fuel, methanol, ethanol [1–3]. The preferred methods in converting hydrocarbons into hydrogen rich synthesis gas are steam reforming, catalytic partial oxidation and autothermal reforming [2]. Carrying out the mentioned reactions under mild conditions (lower temperature and pressure) requires convenient catalysts. The most widely used industrial catalyst is based on Ni. Although Ni is inexpensive with respect to noble metals and offers high activity in reforming reactions, there may be a risk for deactivation through carbon deposition on catalyst surfaces [4–6]. There are several studies concerning elimination of carbon formation during reforming reactions of hydrocarbons and increasing the activity and stability of these catalysts by using different oxide supports, promoters and secondary metal addition. Using CeO_2 as a promoter or support inhibits carbon formation owing to its ability to act as an oxygen buffer by storing/releasing oxygen due to the Ce^{4+}/Ce^{3+} redox couple [4, 7–13].

Another factor influencing the reaction yield is the reactor type choice. Packed bed reactors are used in most industrial processes, however this type of reactors poses challenges in terms of sintering, pressure drop, and preferential path toward the bed. To avoid the disadvantages of packed bed reactors, monolithic reactors can be favored. The benefits of utilising monolithic reactors are short contact time, reduced pressure drop over the reactor length, compact structure, ease of use and easy handling [4, 14–17].

In this paper, addition of Ce as a promoter onto high surface area Al_2O_3 layer and using Co and Pt as secondary catalytic active metals along with Ni on ceramic monolithic structures is discussed in terms of structural characterization.

2. Experimental

2.1. Catalyst preparation

Square channelled cordierite ceramic honeycomb monoliths (Rauschert Technical Ceramics) with cell densities of 400 cpsi were used as primary support for main catalyst components. Monolithic blocks were cut in 20×13 mm^2 ($L \times D$) diameter to obtain cylindrical shapes and were cleaned with acetone before use. $Al(NO_3)_3{\cdot}9H_2O$ (ABCR GmbH), $Ce(NO_3)_3{\cdot}6H_2O$ (ABCR GmbH), $Ni(NO_3)_2{\cdot}6H_2O$ (Carlo Erba), $Co(NO_3)_2{\cdot}6H_2O$ (Carlo Erba), H_2PtCl_6 (8 wt% sol., Sigma Aldrich) were used for preparation of support and catalytic phases.

Catalysts have been synthesized according to dip-coating method. Prior to coating with catalytic components, an Al_2O_3 layer was washcoated on cordierite honeycomb monoliths using $Al(NO_3)_3{\cdot}9H_2O$ solution. Washcoating procedure was repeated to obtain a final average 9 wt% of Al_2O_3 layer on ceramic supports. After drying (for 1 h) at 120 °C in an oven, the Al_2O_3 loaded monoliths were calcined at 600 °C (for 2 h) under static air. Afterwards CeO_2 was added as a promoter over the Al_2O_3 layer by using appropriate concentration of $Ce(NO_3)_3{\cdot}6H_2O$ solution by the same procedure and the sample was calcined at 500 °C (for 2 h). The monoliths were dried at 120 °C for 1 h. Finally Ni, NiCo, PtNi metals were loaded onto washcoated supports to

*corresponding author; e-mail: nguldal@gmail.com

add the catalytic phases. For this purpose, appropriate amounts of $Ni(NO_3)_2{\cdot}6H_2O$, $Co(NO_3)_2{\cdot}6H_2O$, H_2PtCl_6 were mixed with deionized water to obtain a Ni:Co molar ratio of 1 and washcoated supports were dipped into this solution several times until desired amounts of weight gain were achieved. After drying for 1 h at 120 °C, calcination of metal phases took place at 800 °C (for 4 h) under static air for both monometal and binary metal catalysts (5 °C/min heating rate was applied in all calcinations).

The synthesized catalysts: Ni/Al_2O_3, Ni/CeO_2–Al_2O_3, $NiCo/CeO_2$–Al_2O_3, $PtNi/CeO_2$–Al_2O_3 are denoted here as M–A, M–CA1, M–CA2, M–CA3, respectively, where M stands for cordierite monolith, A stands for Al_2O_3, and C stands for CeO_2.

2.2. Characterization

Structural characteristics of the catalysts were investigated by X-ray diffraction (XRD), Brunauer–Emmett–Teller (BET), scanning electron microscopy–energy dispersive spectroscopy (SEM-EDS) and inductively coupled plasma optical emission spectrometry (ICP-OES) techniques. Crystal structure and crystallographic parameters were identified by XRD analyses. XRD analyses were carried out using a Philips Panalytical X'Pert-Pro diffractometer in a diffraction angle range of 10° to 90° with Cu K_α radiation (λ = 0.15418 nm) at operating parameters of 40 mA and 45 kV with a step size of 0.02° and speed of 1°/min.

Specific surface area of the catalysts were measured by employing the BET technique under N_2 as adsorptive gas at 77 K after outgassing at 473 K, using Quantachrome Autosorb Automated Gas Sorption System BET Instrument. Surface morphology and microstructure of the synthesized catalysts were examined by use of field-emission gun scanning electron microscopy (CamScan Apollo 300 FEG-SEM equipment) and semi-quantitative elemental analyses were carried out through X-ray energy dispersive spectroscopy (Oxford EDS apparatus). ICP-OES measurements were performed using Perkin Elmer Optima 2100 DV to quantify metal contents present in the samples.

2.3. Results and discussion

2.3.1. XRD results

XRD patterns of the structured catalysts and lattice constants are given in Fig. 1 and Table I, respectively. NiO, CoO and Co_3O_4 phases exist in cubic crystal structures. Characteristic CeO_2 fluorite structure is observed in Ni/CeO_2–Al_2O_3, $NiCo/CeO_2$–Al_2O_3, and in $PtNi/CeO_2$–Al_2O_3. Al_2O_3 phase exists as rhombohedral in three catalysts, though hexagonal crystal structure is found in $NiCo/CeO_2$–Al_2O_3. Platinum occurs as PtO in tetragonal structure. Since it is coating of metal oxides (< 5 wt%) on cordierite support ($Mg_2Al_4Si_5O_{18}$), the XRD peaks corresponding to cordierite structure are dominant. The peaks corresponding to $NiAl_2O_4$ spinel, Co_2NiO_4, $CoNiO_2$, $CeAl_{11}O_{18}$, $CeAlO_3$ phases may exist, however they are not clearly visible due to their low amounts with respect to cordierite and other phases.

TABLE I

Crystal structures of synthesized catalysts.

Catalyst	Phases	Reference code	Crystal system	Space group	a, b, c [Å]	α, β, γ [°]
M–A	Al_2O_3	01-077-2135	rhombohedral	R-3c	4.7606, 4.7606, 12.994	90, 90, 120
	NiO	01-089-7130	cubic	Fm-3m	4.1944, 4.1944, 4.1944	90, 90, 90
M–CA1	Al_2O_3	01-077-2135	rhombohedral	R-3c	4.7606, 4.7606, 12.994	90, 90, 120
	CeO_2	01-081-0792	cubic	Fm-3m	5.4124, 5.4124, 5.4124	90, 90, 90
	NiO	01-089-5881	cubic	Fm-3m	8.3532, 8.3532, 8.3532	90, 90, 90
M-CA2	Al_2O_3	00-021-0010	hexagonal	P E	7.8490, 7.8490, 16.183	90, 90, 120
	CeO_2	00-001-0800	cubic	Fm-3m	5.4100, 5.4100, 5.4100	90, 90, 90
	NiO	01-089-5881	cubic	Fm-3m	8.3532, 8.3532, 8.3532	90, 90, 90
	CoO	00-001-1227	cubic	Fm-3m	4.2400, 4.2400, 4.2400	90, 90, 90
	Co_3O_4	01-073-1701	cubic	Fd-3m	8.0835, 8.0835, 8.0835	90, 90, 90
M–CA3	Al_2O_3	00-003-1033	rhombohedral	R-3c	4.7510, 4.7510, 12.970	90, 90, 120
	CeO_2	00-001-0800	cubic	Fm-3m	5.4100, 5.4100, 5.4100	90, 90, 90
	NiO	01-089-5881	cubic	Fm-3m	8.3532, 8.3532, 8.3532	90, 90, 90
	PtO	01-085-0714	tetragonal	$P42/mmc$	3.0400, 3.0400, 5.3400	90, 90, 90

2.3.2. BET results

According to BET measurements, the highest specific surface area has been attained at $PtNi/CeO_2$–Al_2O_3, however as can be seen (from Table II) that Ni/CeO_2–Al_2O_3 has similar specific surface area when compared to $PtNi/CeO_2$–Al_2O_3. There is no adverse effect of loading 0.04 wt% of Pt into the catalyst $PtNi/CeO_2$–Al_2O_3, on the contrary it led to a slight increase in surface

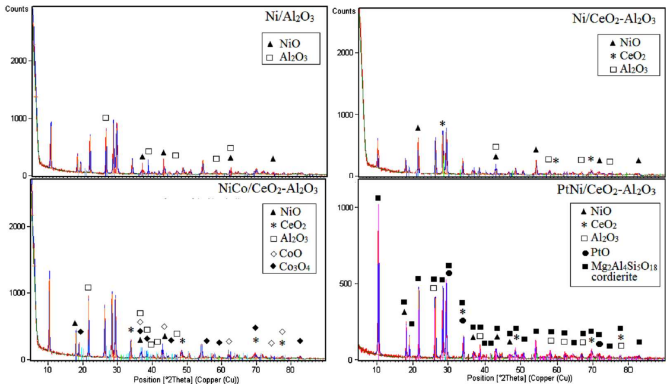

Fig. 1. XRD patterns of synthesized structured catalysts.

area. The addition of Co as a secondary metal in NiCo/CeO_2–Al_2O_3 caused a decrease in surface area when compared with Ni/CeO_2–Al_2O_3. Surface area of PtNi/CeO_2–Al_2O_3 is higher than NiCo/CeO_2–Al_2O_3 even if these two catalysts contain the same number of components (two metals plus two supporting oxides). The probable reason for this is based on the very low quantity of Pt loading. The lowest specific surface area is observed on Ni/Al_2O_3. Regardless, the washcoating procedure of cordierite monolith samples with Al_2O_3 layer increases the specific surface area excessively in comparison with blank cordierite support which is 0.23 m^2/g.

TABLE II

Specific surface areas determined by BET and metal contents determined ICP-OES.

Catalyst	BET surface area [m^2/g]	ICP-OES wt%
Ni/Al_2O_3	7.58	Ni: 0.757
Ni/CeO_2–Al_2O_3	9.57	Ni: 0.53/Ce: 3.88
NiCo/CeO_2–Al_2O_3	8.49	Ni: 0.86/Co: 0.00075/Ce: 4.026
PtNi/CeO_2–Al_2O_3	9.98	Pt: 0.04/Ni: 0.88/Ce: 3.74
blank monolith	0.23	–

2.3.3. ICP-OES results

The results of ICP-OES measurements are listed in Table II. Although the theoretical Ni:Co ratio on weight basis is 1, the ratio according to ICP analyses is different. The amount of the specimen taken randomly for ICP analyses is too low compared to the whole sample to be analysed and the metal contents present after grinding of the ceramic monoliths is not uniform throughout the catalyst powder. This inhomogeneity of the catalyst powders may reveal mismatched results between theoretical and ICP measurements.

2.3.4. SEM-EDS results

The observations of channel internal surfaces (in Fig. 2) demonstrate the differences in morphology between CeO_2 loaded (M–CA1, M–CA2, M–CA3) and unloaded M–A catalysts. In the case of non-doped catalyst, rough surface is visible, whereas relatively smooth surfaces can be seen in CeO_2 doped samples. Although EDS measurements were done, they are not convenient to report here due to difficult measurement of the metal contents accurately for coated samples.

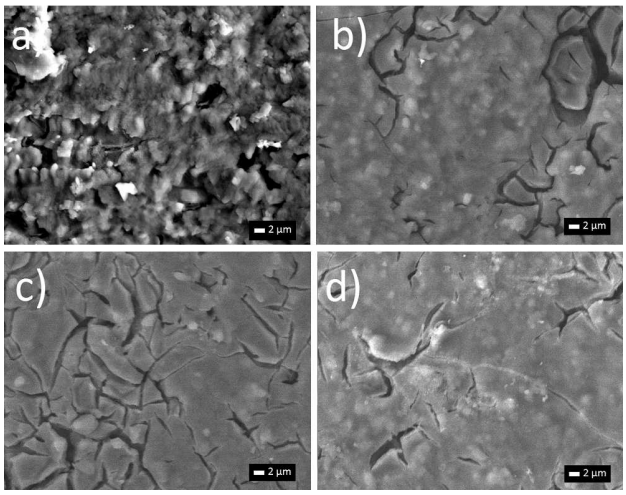

Fig. 2. SEM pictures of structured catalysts. Interior channel surface views of (a) M–A, (b) M–CA1, (c) M–CA2 and (d) M–CA3 in 2000× magnification.

3. Conclusion

Using ceramic monolith to obtain structured catalyst provides primary support, Al_2O_3 layer — the secondary support. Washcoating of cordierite ceramic monoliths with an Al_2O_3 layer remarkably enhances specific surface areas, which is a crucial parameter in catalytic materials. Adding CeO_2 as a promoter hinders carbon formation which occurs on catalyst surfaces during hydrocarbon reforming reactions by acting as an oxygen buffer via storing/releasing oxygen due to the Ce^{4+}/Ce^{3+} redox couple. In the present work, Ni and Co were used as active catalytic components because of their low cost compared to noble metals. Pt was added in low quantities to further enhance catalytic activity. When taking into account the physical properties of chanelled ceramic monoliths used as catalyst supports, there are advantages such as lower pressure drop, laminar flow, ease of use (no need to separate reactants and catalyst particles after reaction), mechanical strength, high resistance to plugging, and compatibility with gas and liquid reactions.

Acknowledgments

Financial supports of Black Sea ERA.NET 2010 Pilot Joint Call (project No. BS-ERA.Net: 028 acronymed as H2S-PROTON) and Yildiz Technical University Research Foundation (project No. 27-07-01-07) and technical assistance of Chemical Engineering Department for SEM-EDS, XRD and ICP-OES analyses and UNIDO-ICHET for BET measurements are gratefully acknowledged.

References

[1] M. Momirlan, T.N. Veziroglu, *Ren. Sust. Energy Rev.* **6**, 141 (2002).

[2] R.M. Navarro, M.A. Pena, J.L.G. Fierro, *Chem. Rev.* **107**, 3952 (2007).

[3] W.S. Harvey, J.H. Davidson, E.A. Fletcher, *Ind. Eng. Res.* **37**, 2323 (1998).

[4] B.C. Enger, R. Lodeng, A. Holmen, *Appl. Catal. A, Gen.* **346**, 1 (2008).

[5] H.W. Kim, K.M. Kang, H.Y. Kwak, J.H. Kim, *Chem. Eng. J.* **168**, 775 (2011).

[6] Z. Xu, Y. Li, J. Zhang, L. Chang, R. Zhou, Z. Duan, *Appl. Catal. A, Gen.* **210**, 45 (2001).

[7] X. Cai, X. Dong, W. Lin, *J. Natural Gas Chem.* **17**, 98 (2008).

[8] S. Damyanova, J.M.C. Bueno, *Appl. Catal. A, Gen.* **253**, 135 (2003).

[9] S. Wang, G.Q. Lu, *Appl. Catal. B, Env.* **19**, 267 (1998).

[10] A.C.W. Koh, L. Chen, W.L. Leong, B.F.G. Johnson, T. Khimyak, J. Lin, *Int. J. Hydrogen Energy* **32**, 725 (2007).

[11] J. Zhang, H. Wang, A.K. Dalai, *J. Catalysis* **249**, 300 (2007).

[12] M.M.V.M. Souza, O.R.M. Neto, M. Schmal, *J. Natural Gas Chem.* **15**, 21 (2006).

[13] L.V. Mattos, F.B. Noronha, *J. Power Sources* **145**, 10 (2005).

[14] V. Meille, *Appl. Catal. A, Gen.* **315**, 1 (2006).

[15] T.A. Nijhuis, A.E.W. Beers, T. Vergunst, I. Hoek, F. Kapteijn, J.A. Moulijn, *Catal. Rev.* **43**, 345 (2001).

[16] C.P. Rodrigues, M. Schmal, *Int. J. Hydrogen Energy* **36**, 10709 (2011).

[17] T. Giroux, S. Hwang, Y. Liu, W. Ruettinger, L. Shore, *Appl. Catal. B, Env.* **56**, 95 (2005).